SA21A-09

The Relationship Between the Enhanced Aurora and Thin, Dense Ionization Layers

Jay R. Johnson

Hideo Okuda

Princeton University, Plasma Physics Laboratory

Spring AGU Meeting
May 24, 2004

PPPL
PRINCETON PLASMA PHYSICS LABORATORY

Observations of Enhanced Aurora

Observations of Enhanced Aurora

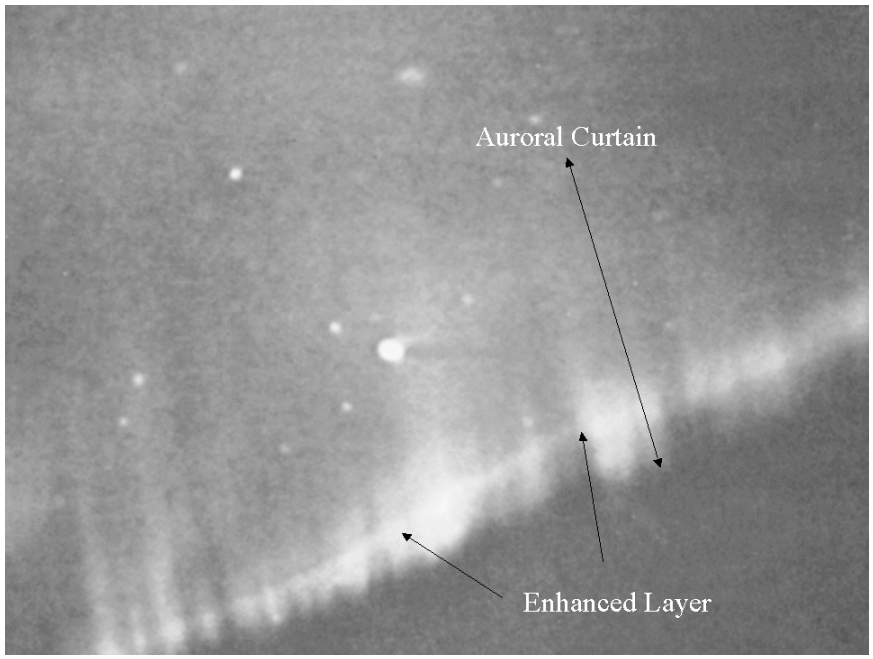

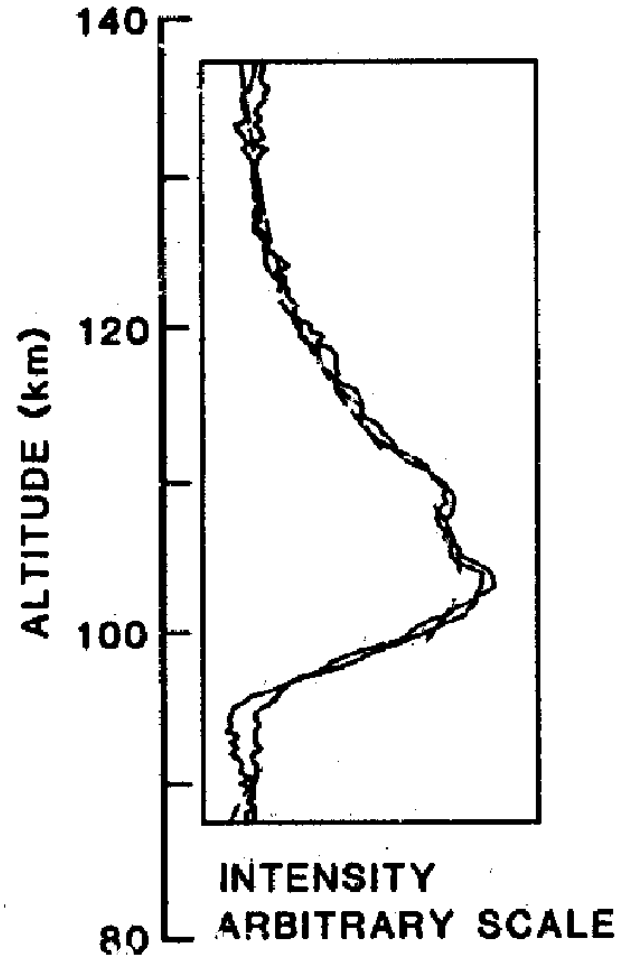

[Hallinan et al., 1985]

Properties of Enhanced Aurora

- Altitude
  - 90-130km
- Thickness
  - typical 1km
  - range up to 5-15km
- Intensity
  - Up to 5:1
- Multiple Layers
- Profile not consistent with collisional electron precipitation models

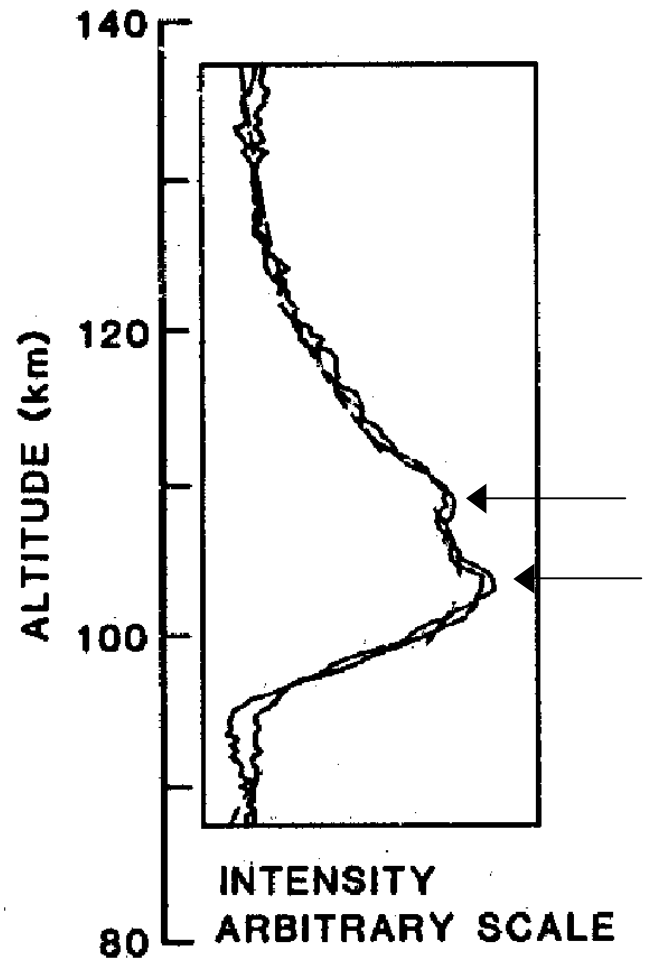

[Hallinan et al., 1985]

Dynamics of Enhanced Aurora

- Stable
  - Remain 1-2 hours
- Active Times
  - Layer remains at fixed altitude even when precipitation extends to lower altitude
  - E.g. lower border ⇒ enhanced layer

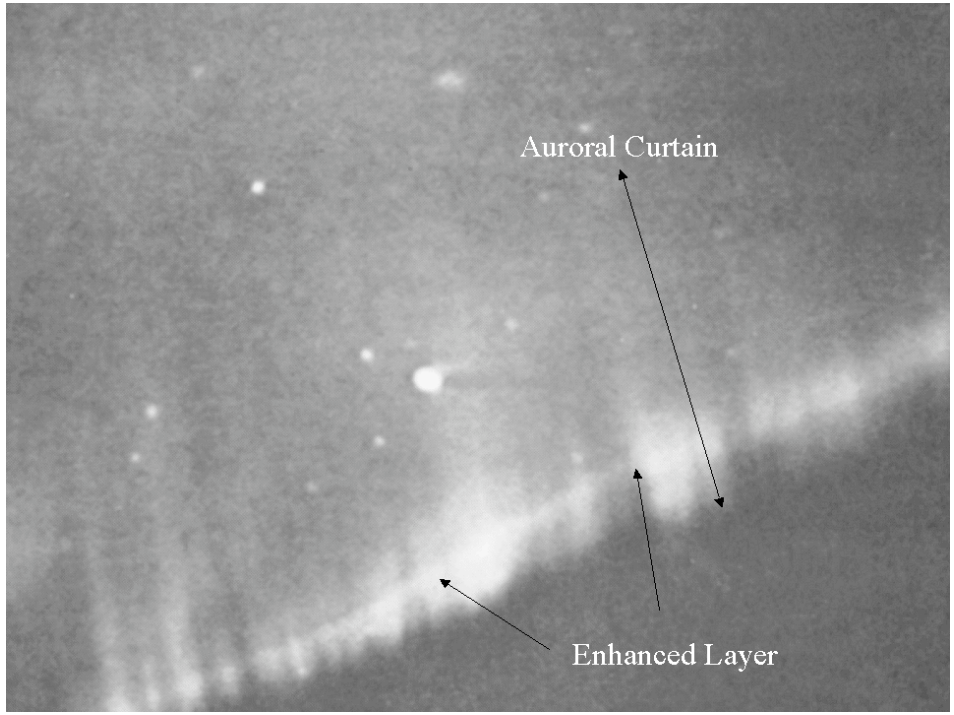

[Hallinan et al., 1985]

Optical Emissions and Energetic Electrons

- All luminosity bands enhanced
- 4278Å N_2^+ band
  - ⇒electrons must have energies above ionization energy of N_2 (17 eV)

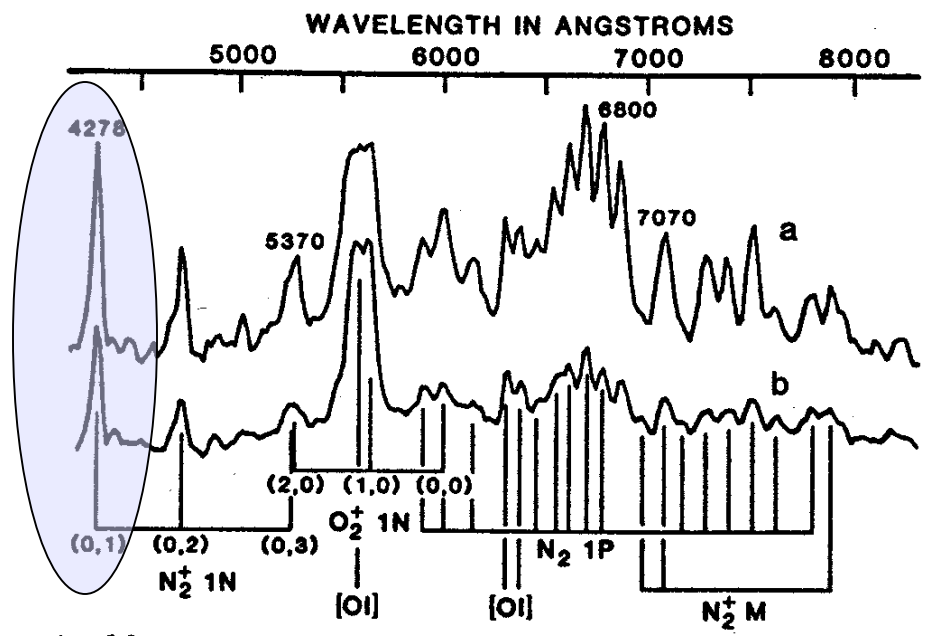

N_2 Ionization Cross Section

- Ionization energy for molecular nitrogen around 17eV.
- Peak ionization around 100eV

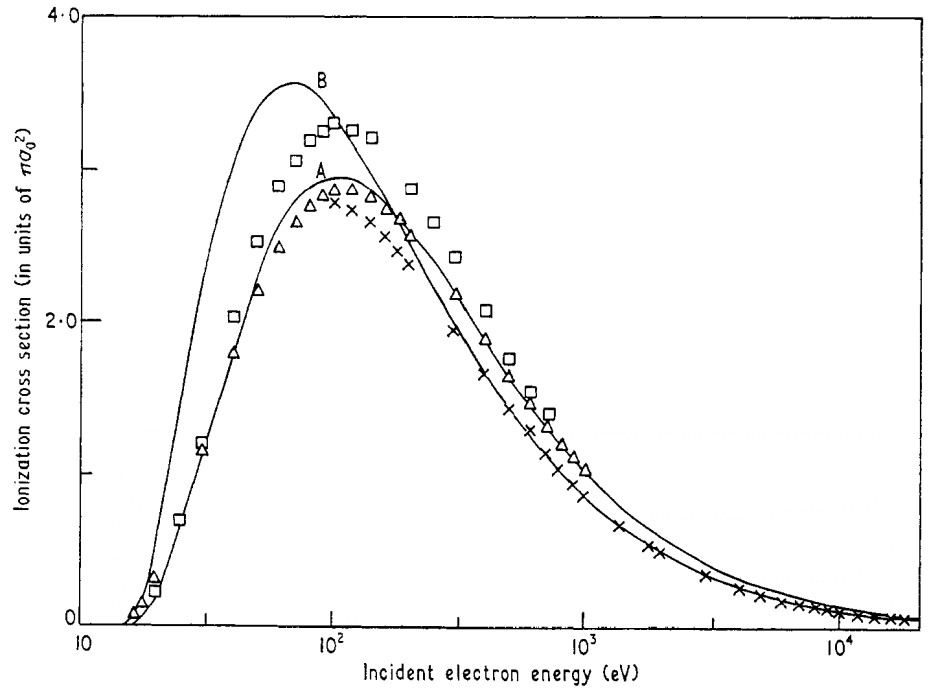

Figure 2. Electron impact ionization of molecular nitrogen. Theoretical cross sections: curve A, present calculation; curve B, results obtained using formula (15) of Vriens 1965. Experimental cross sections: □ Tate and Smith 1932; △ Rapp and Englander-Golden, 1965; × Schram *et al.* 1965, 1966.

Optical Emissions and Energetic Electrons

- O, N_2 bands are significantly enhanced
- N_2^+ emissions suppressed
  - indicates that at times the electron energy does not exceed the N_2^+ ionization energy
- e^- energy ~ 10-20 eV with sharp cutoff above 20 eV

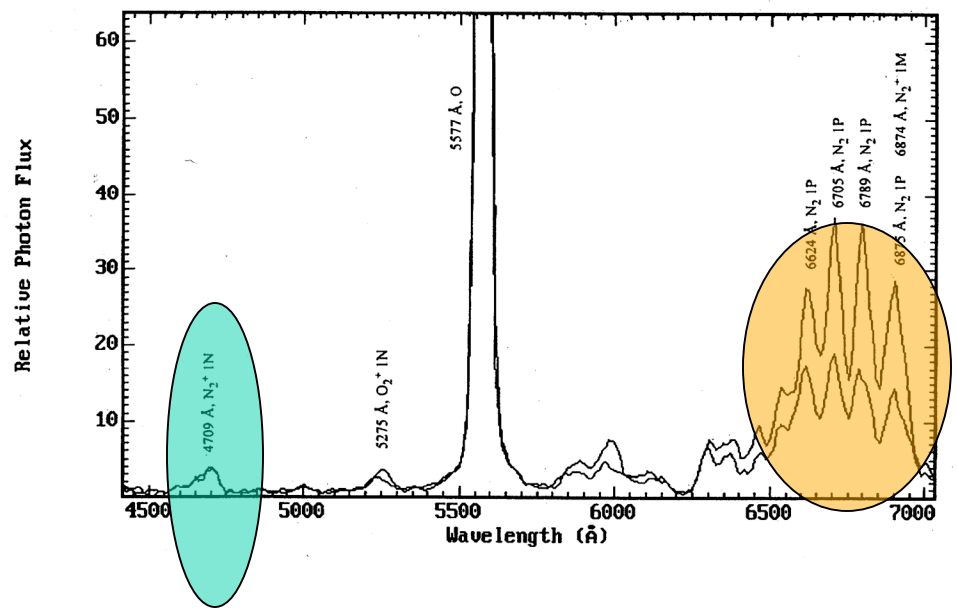

Two Conclusions

- The atmosphere in the auroral zone contains one or more very thin stable layers that may interact with precipitating electrons and auroral currents.
- Because collisional models for electron precipitation cannot produce such thin layers, it is likely that a collective plasma process energizes electrons in the layers.

Thin Ionization Layers Observed

- Incoherent-scatter radar detects thin layers of electrons
- Layer around 110 km during 2105-2120 UT on 7/27/1991
- Layer remained for two hours 2000-2200 UT
- Thickness between 1.5 and 2.5 km
- Density peak between 10^5 and 10^6 cm^{-3}

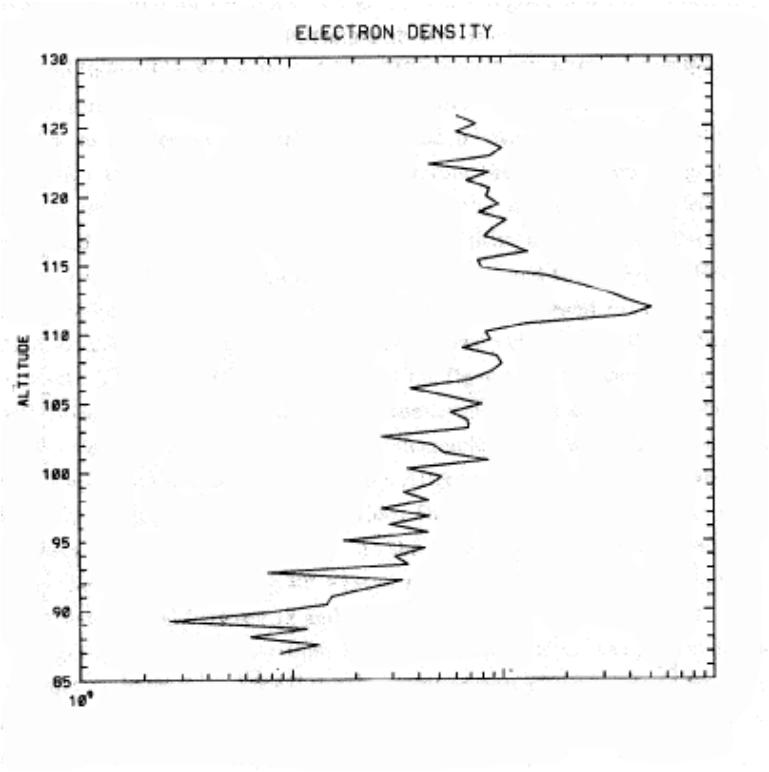

Bristow and Watkins, 1993

Formation of Layers

- Neutral Winds (at low latitude)
- Electric Fields (at high latitudes)

[Nygren, 1984]

$$q(\mathbf{E} + \mathbf{v} \times \mathbf{B}) - m_i \nu_{in}(\mathbf{v} - \mathbf{u}) = 0 \qquad (3)$$

$$v_{iz} = \frac{E/B}{1 + b^2}(b \cos\phi - \sin\phi) \cos\theta \qquad (4)$$

where $b \equiv \nu_i / \Omega_i$, θ is the dip angle with respect to the vertical, and the electric field makes an angle ϕ with respect to northward.

Convergence of Ion Flows

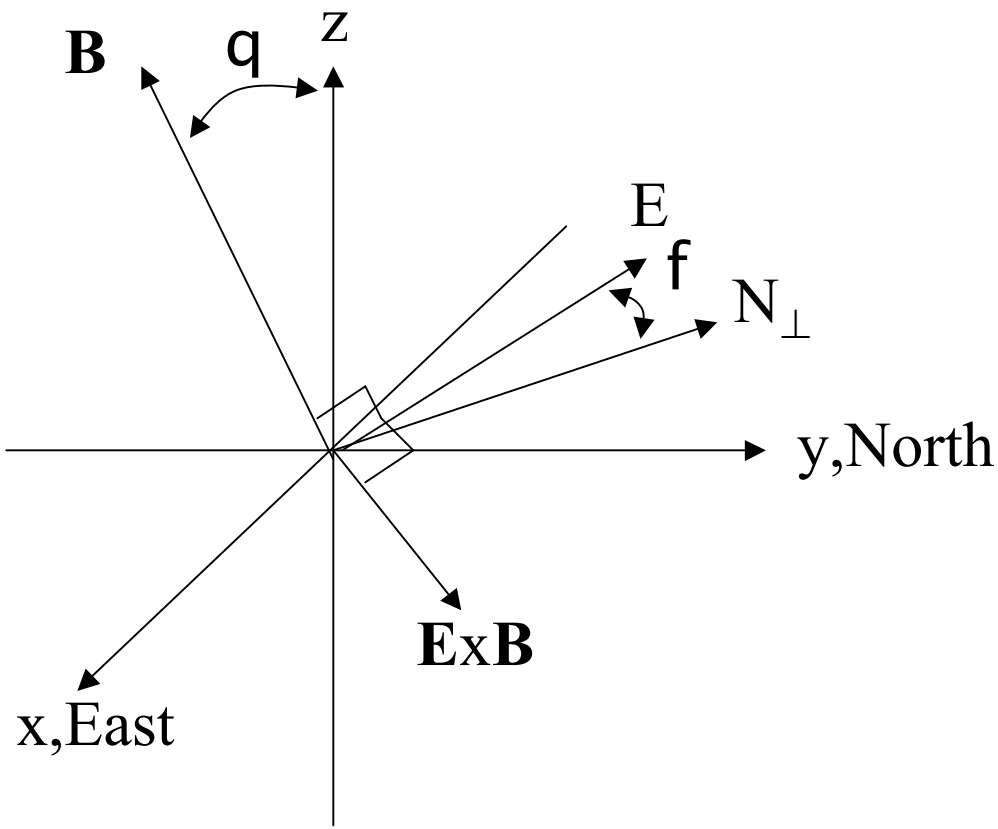

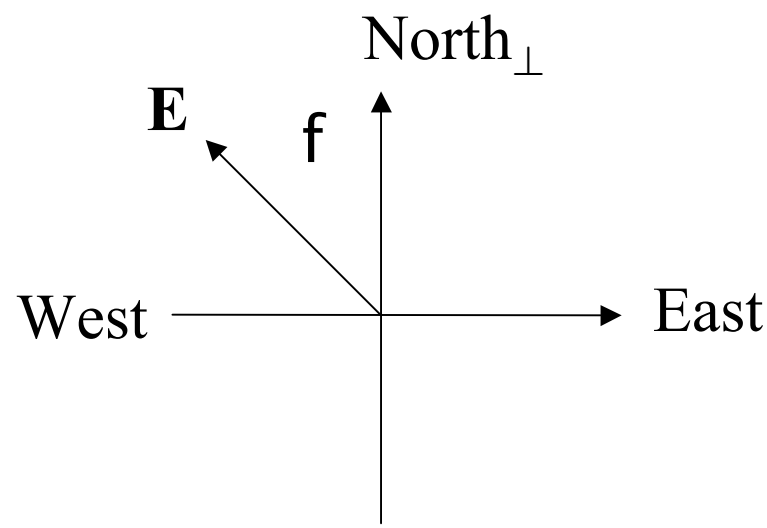

Formation of Thin Layers

- Metallic ions originate from meteor ablation, [Kelley, 1989]
- Fe^+ and Mg^+ have been observed in abundance by rocket and incoherent scatter radar

  [Narcisi et al., 1968, Turunen et al., 1988]
- Ion accumulation occurs for different electric field orientations

  [Nygren et al., 1984]

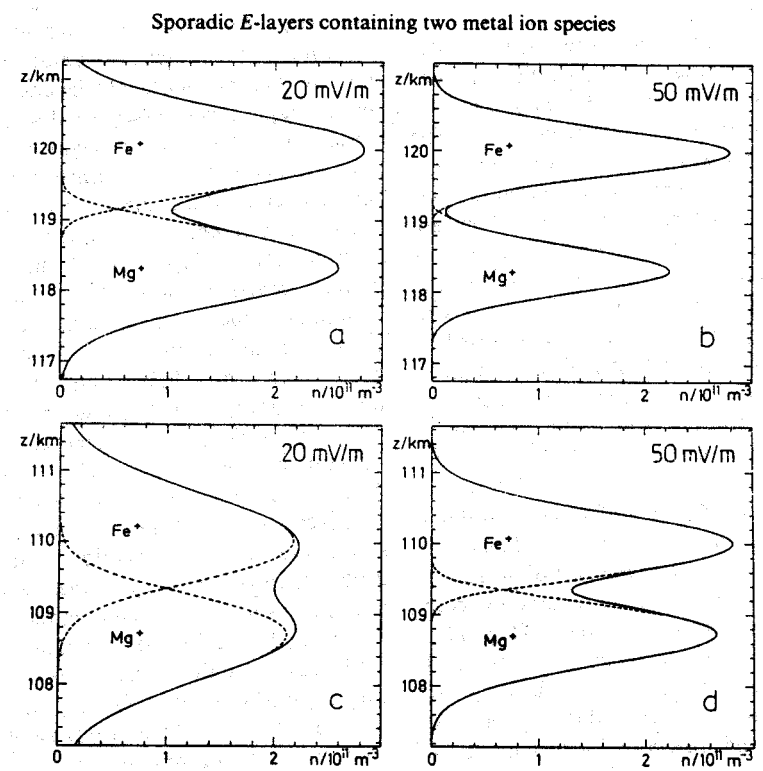

Possible Mechanisms

- Beam Plasma Discharge
  - Electron beam source
  - Emission spectra similar to enhanced aurora spectrum
  - Discharge does not result from a special gas layer
  - Location depends on beam current ?
  - Does not explain the aurora below the enhanced layer ?

  [Bernstein et al., 1978; Hallinan et al., 1988]
- Ionization Instability
  - Would be confined to the lower edge ?

  [D'Angelo, 1991]

Possible Mechanisms

- Upper Hybrid and Electron Cyclotron Instability
  - Layers could be localized by maxima in the growth rate at cyclotron harmonics
  - Localization depends on electron energy and may be variable during precipitation

  [Basu et al., 1982; Chang and Jasperse, 1992]
- DC electric field

  [Shepherd and Falthammer, 1980]

Modified Two-Stream Instability

- Cross Field Current
  - In E/F region $\nu_{in} > \Omega_i$

    but $\nu_{en,ei} < \Omega_e$
- Hence a cross field current can be produced by an ionospheric electric field
- Dispersion Relation in electron frame (U ~ ExB)

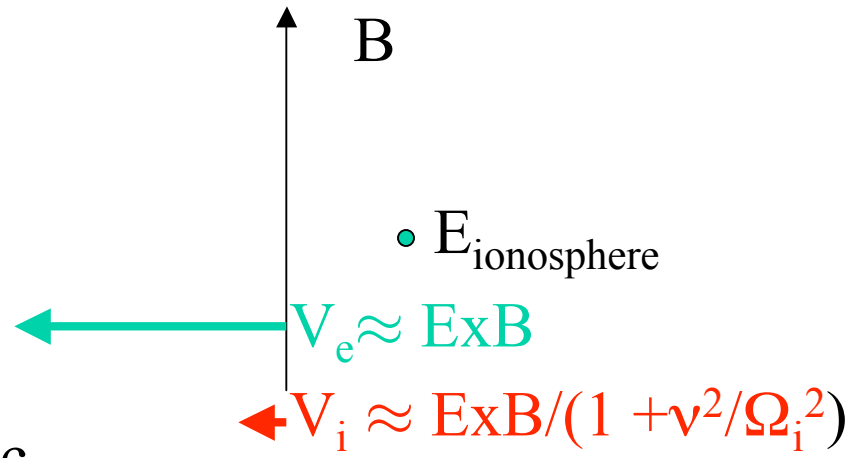

$$1+\frac{k_\perp^2}{k^2}\left(\frac{\omega_{pe}^2}{\Omega_{ce}^2}\frac{(\omega+i\nu_e)}{\omega}-\frac{\omega_{pi}^2}{(\omega-\mathbf{k}\cdot\mathbf{U})(\omega-\mathbf{k}\cdot\mathbf{U}+i\nu_i)}\right)-\frac{k_\parallel^2}{k^2}\frac{\omega_{pe}^2}{\omega(\omega+i\nu_e)}=0 \quad (1)$$

Modified Two-Stream Instability

[McBride et al., 1972]

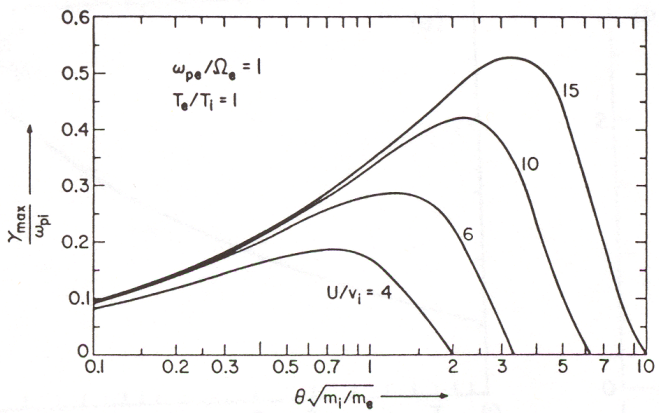

FIG. 2. Plots of the maximum growth rate normalized to ω_{pi} vs $\theta(m_i/m_e)^{1/2}$ for a hydrogen plasma for different values of U/v_i.

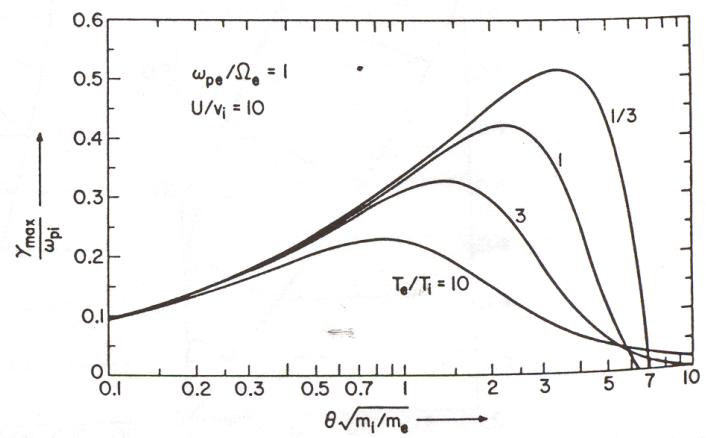

FIG. 3. Plots of the maximum growth rate normalized to ω_{pi} vs $\theta(m_i/m_e)^{1/2}$ for a hydrogen plasma for different values of T_e/T_i.

- $v_{thi} = T / m_i$
- $V_{Fe+} < V_{N2+,NO+} < U$
- increased instability in thin layer

- electron Landau damping stabilizes plasma

Growth Rate Enhanced in the Thin, Dense, Heavy Ion Layer

Species	mass	density (cm^{-3})	γ (kHz)
Fe^+	56	10^6	11
Mg^+	24	10^6	16
O_2^+	32	10^5	4
NO^+	30	10^5	5

Global Eigenmode Analysis

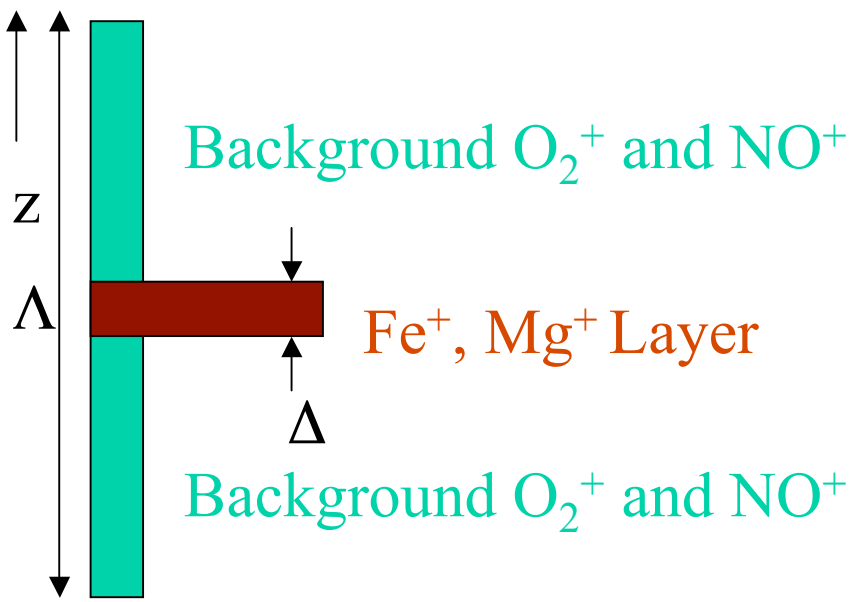

$$\frac{d^2\phi}{dz^2} = -k_{\parallel}^2(z)$$

The eigenfunctions in the slab geometry are sinusoids which obey an eigenvalue condition

$$k_2 \tan(k_1(\Lambda - \Delta)/2) + k_1 \tan(k_2\Delta/2) = 0 \quad (1)$$

for the even modes and

$$k_2 \tan(k_1(\Lambda - \Delta)/2) - k_1 \cot(k_2\Delta/2) = 0 \quad (2)$$

for the odd modes. The wavevectors, k_1 and k_2 are the solutions of $d^2\phi/dz^2 = k_{1,2}^2\phi$ in the background (1) and thin layer (2) regions respectively. These equations may be solved to provide a discrete spectrum $\omega_j(k_y)$. The solutions in the two regions are sinusoids.

$$k_{\parallel}^2\left(1 - \frac{\omega_{pe}^2}{\omega(\omega + i\nu_e)}\right) = -k_{\perp}^2\left(\frac{\omega_{pe}^2}{\Omega_{ce}^2}\frac{(\omega + i\nu_e)}{\omega} - \frac{\omega_{pi}^2}{(\omega - \mathbf{k}\cdot\mathbf{U})(\omega - \mathbf{k}\cdot\mathbf{U} + i\nu_i)}\right)$$

Global Eigenmode Analysis

- Growth rates are discrete versions of the continuous dispersion relation with

$$k_{\parallel} \sim (n+\tfrac{1}{2})\pi/\Lambda$$

- The thin layer introduces new modes with larger growth rate
- The heavy ion modes are localized in the heavy ion layer

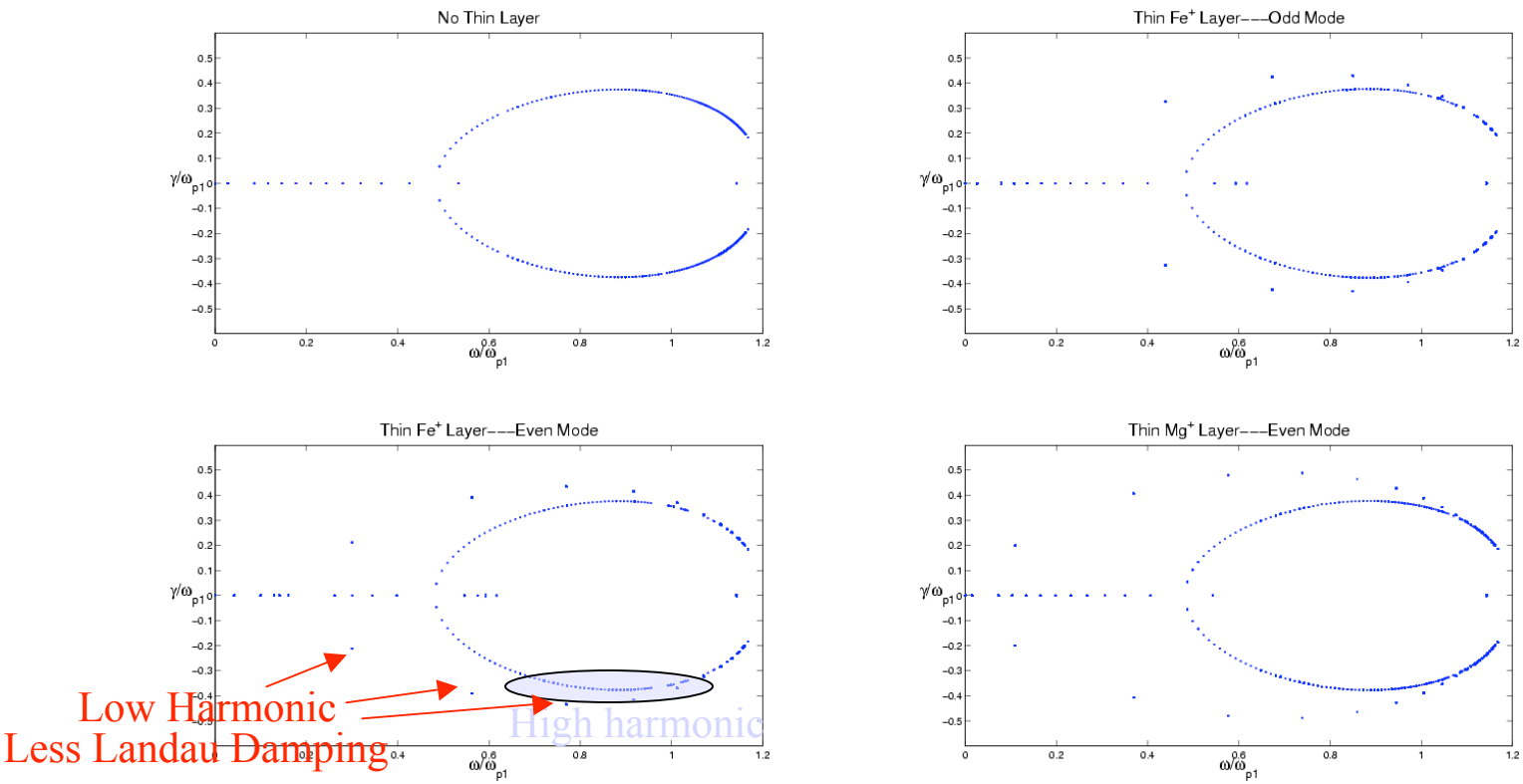

Effect of Collisions

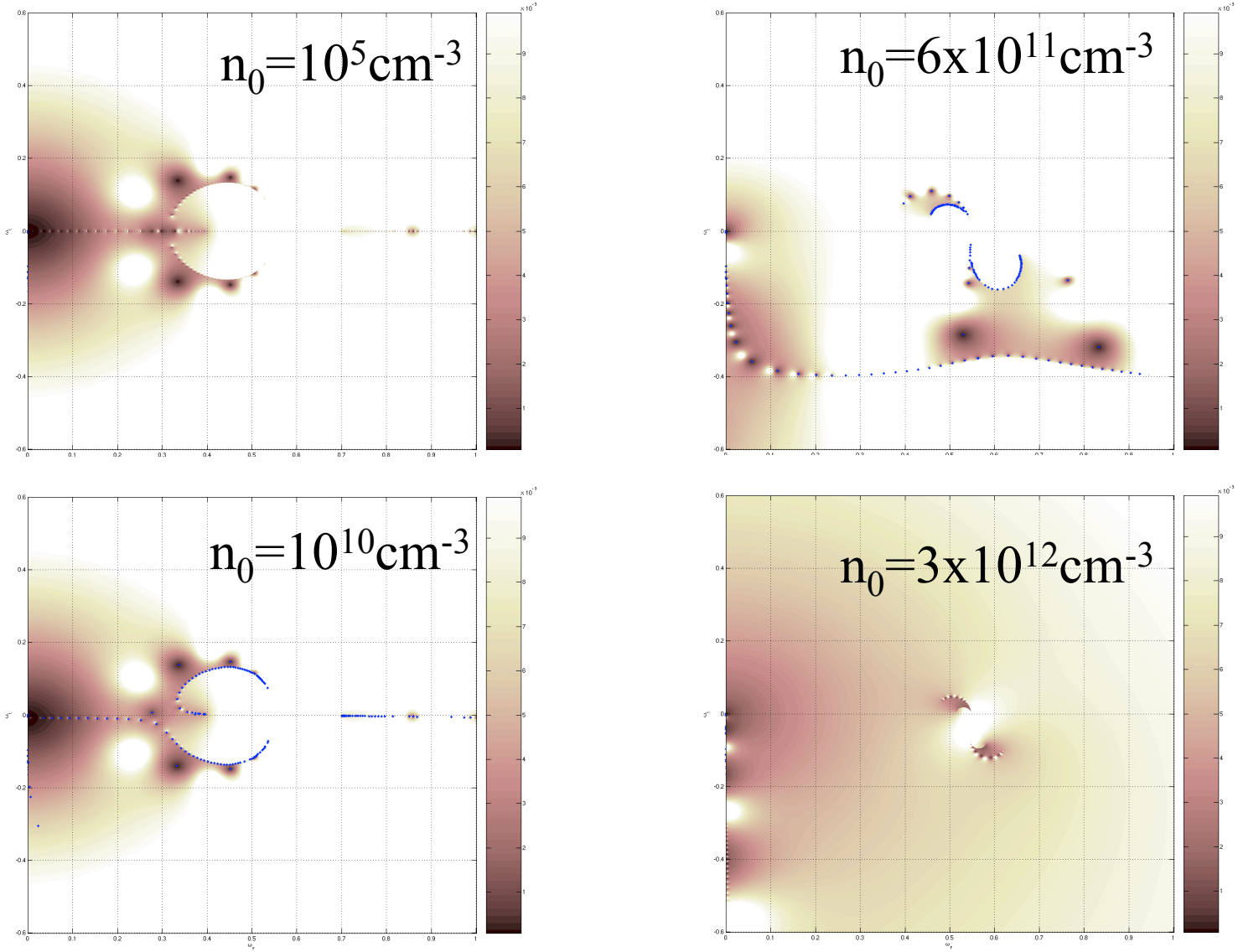

Reasons to Expect Mode Even More Unstable in Thin Layer

- Threshold drift speed is smaller in the layer because v_{ti} is smaller
- Maximum growth rate is larger in the layer where v_{ti} is smaller
- Electron thermal effects stabilize the instability for large $k_{\|}$. Maximum stability occurs where $q = \tan^{-1}(k_{\|} / k_{\perp}) \sim (m_e/m_i)^{1/2} \Rightarrow$ heavy ions instability is less oblique and suffers less electron Landau damping at the same $k_{\perp}$

Simulation Method

- 2 ½ D Simulation Code [Okuda and Lee, 1978]
- Guiding center electrons
- Fe^+ ions ACTUAL

  $m_i / m_e = 102{,}827$
- $U = 10\ v_{thi}$

  ExB 1V/m E field
- BC: Dirichlet x, Periodic y
- Run for $\omega_{pe}t=24000$

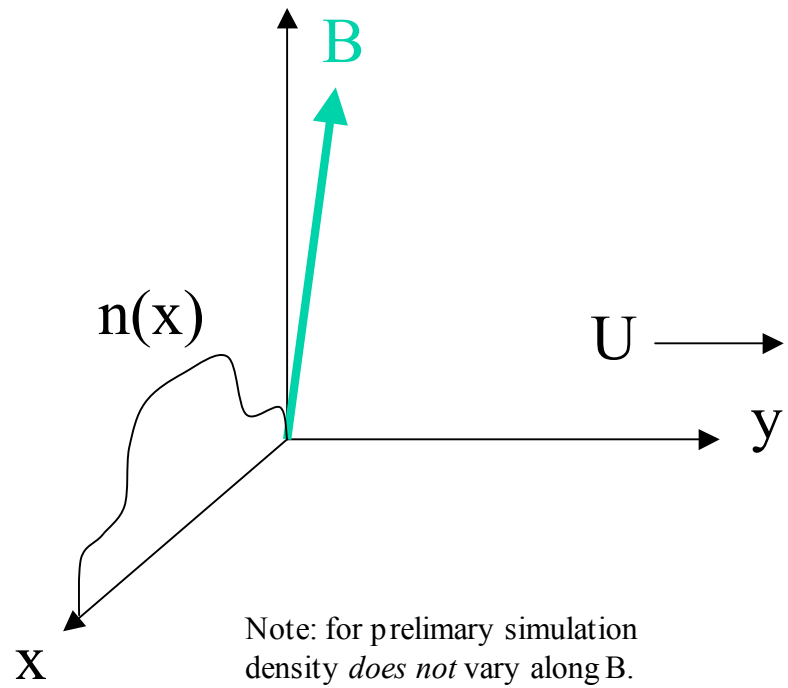

Note: for prelimary simulation density *does not* vary along B. This would require collisions to stabilize the simulation. This simulation demonstrates:

(a) Heavy ion layer is more unstable

(b) Electrons can be significantly heated

Electron-Neutral Collisions

- Electron neutral collisions [Lummerzheim, 1987]

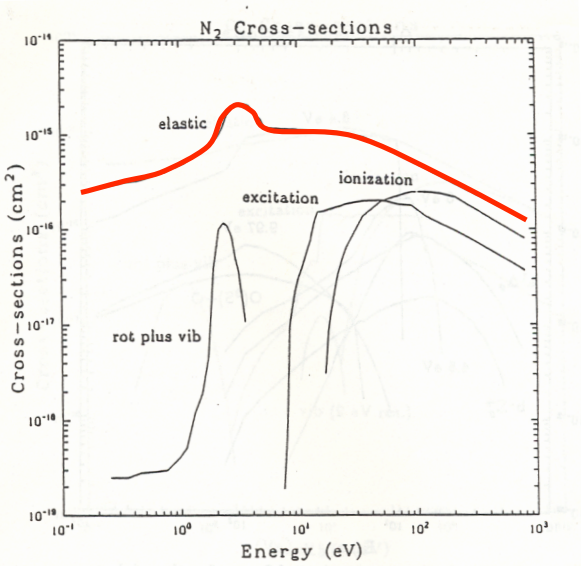

Fig. 2.2a Elastic, ionization, vibrational excitation, and the sum of all excitation cross sections of N_2 as a function of electron impact energy.

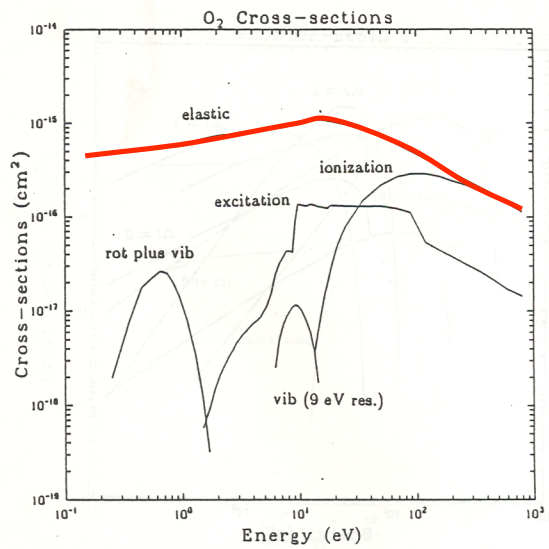

Fig. 2.2b Elastic, ionization, vibrational excitation, and the sum of all excitation cross sections of O_2 as a function of electron impact energy.

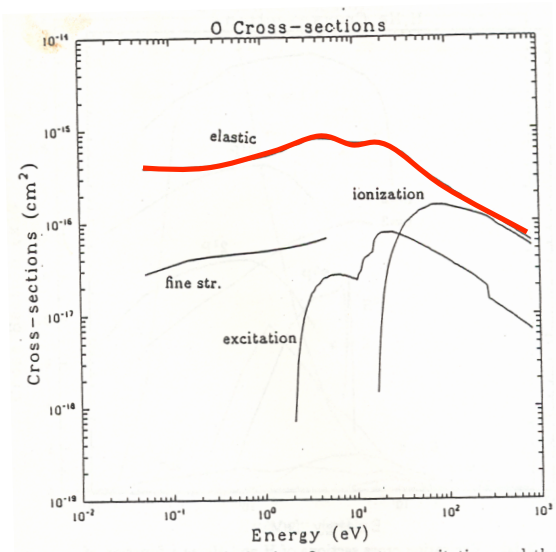

Fig. 2.2c Elastic, ionization, fine structure excitation, and the sum of all excitation cross sections of O as a function of electron impact energy.

Electron-Neutral Collisions

- Assume elastic collisions that preserve energy with $\sigma \sim 10^{-15}$ cm^2
- The collision frequency is given by

$$\nu_e = n_0 \, \sigma^{e/O} \, v_e$$

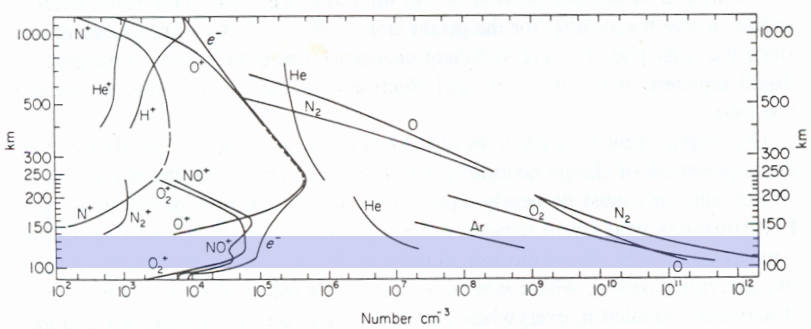

Fig. 1.2. International Quiet Solar Year (IQSY) daytime atmospheric composition, based on mass spectrometer measurements above White Sands, New Mexico (32°N, 106°W). The helium distribution is from a nighttime measurement. Distributions above 250 km are from the Elektron II satellite results of Istomin (1966) and Explorer XVII results of Reber and Nicolet (1965). [C. Y. Johnson, U.S. Naval Research Laboratory, Washington, D.C. Reprinted from Johnson (1969) by permission of the MIT Press, Cambridge, Massachusetts. Copyright 1969 by MIT.]

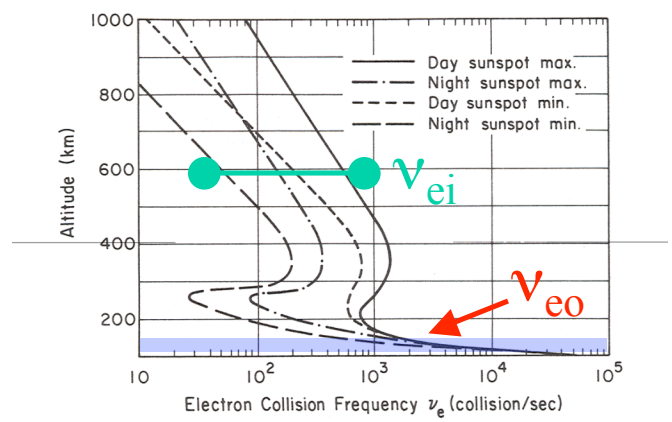

Fig. B.3. Electron collision frequency versus altitude. [From Johnson (1961).]

Ion Collisions

- Assume hard sphere collisions with cross section $\sigma^{\alpha/0} \sim 5 \times 10^{15}$ cm^{-2}.
- Collsion frequency $\nu_\alpha = n_0 \, \sigma^{\alpha/0} \, v_\alpha$ for collisions of species (α) with neutral species (0)

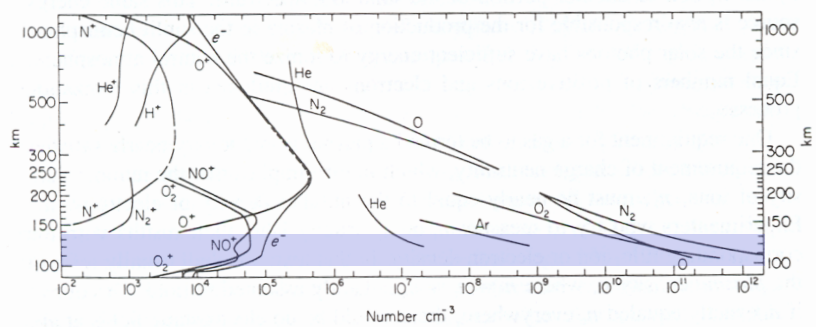

Fig. 1.2. International Quiet Solar Year (IQSY) daytime atmospheric composition, based on mass spectrometer measurements above White Sands, New Mexico (32°N, 106°W). The helium distribution is from a nighttime measurement. Distributions above 250 km are from the Elektron II satellite results of Istomin (1966) and Explorer XVII results of Reber and Nicolet (1965). [C. Y. Johnson, U.S. Naval Research Laboratory, Washington, D.C. Reprinted from Johnson (1969) by permission of the MIT Press, Cambridge, Massachusetts. Copyright 1969 by MIT.]

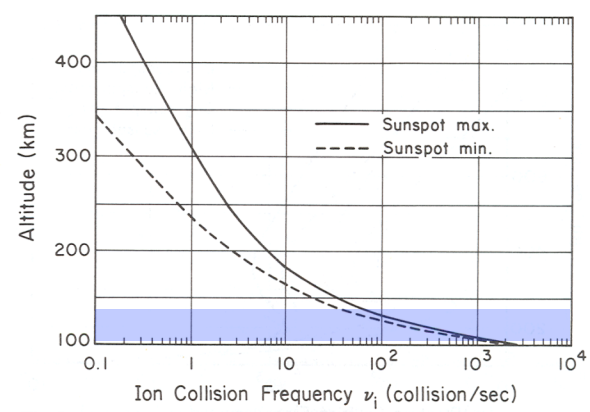

Fig. B.2. Ion collision frequency versus altitude. [From Johnson (1961).]

Collisional Method

- At each time step compute probability for a collision to occur for a particle with velocity v and apply randomly according to a Poisson distribution.
- For electrons, conserve energy, but randomize pitch angle.
- For ions, replace an ion that collides with a new particle from the thermal background (0.3 eV) used to intialize the simulation.

Comparison of Electron and Ion Collisions

- For perpendicular dynamics:
  - $\kappa \sim 1/[(\omega + i\,\nu_j)^2 - \Omega_j^2]$
    - For electrons: $\omega << \nu_e << \Omega_e$
    - For ions: $\nu_I \sim \omega \sim \Omega_i$
- For parallel dynamics
  - $\kappa \sim \omega_{pj}^{\,2} / (\omega + i\,\nu_j) \sim 4\pi n_j e^2/(n_O\,\sigma^2\,T_j)$
  - All species are important

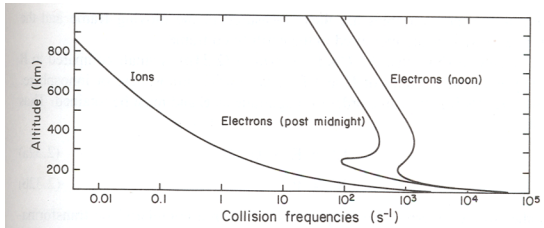

Fig. 2.3. Typical electron and ion–neutral collision frequencies at high sunspot number. [From "Satellite Environment Handbook," edited by F. Johnson (1961). Reproduced by permission of Stanford Univ. Press. Copyright © 1961 by the Board of Trustees of the Leland Stanford Junior University.]

Electrostatic Particle Simulation

- Initial Conditions

Ion Density $n_i(x)$

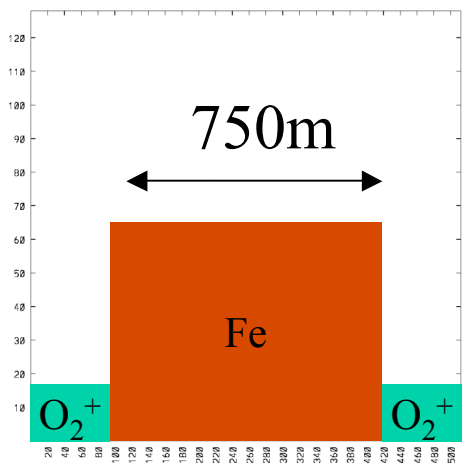

x / ρ_e

Electron Parallel Distribution $f_e(v_{\|})$

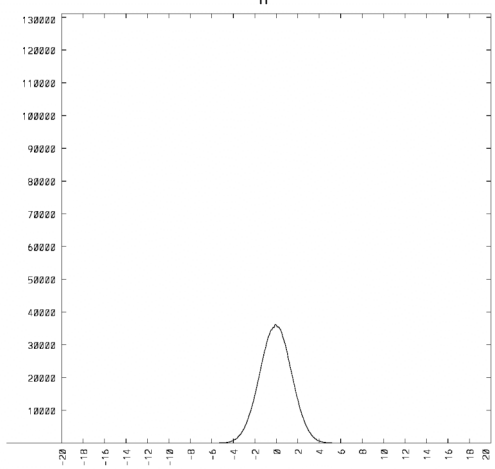

$v_{\|} / v_{te}$

Ion Perpendicular Distribution $f_i(v_{\perp})$

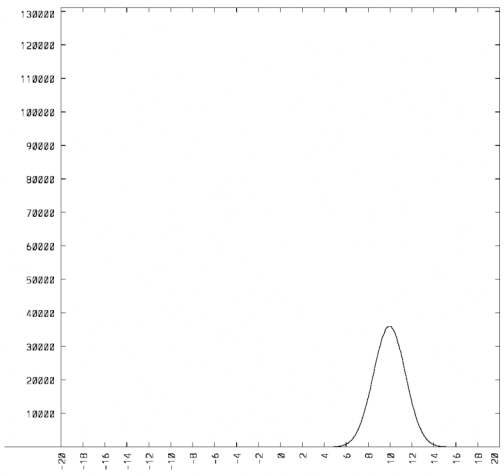

v_y / v_{ti}

$\rho_e = c/\omega_{pe}$; $\rho_i = 64\ \rho_e = 15\text{m}$

Electrostatic Particle Simulation

- Simulation at $\omega_{pe}t = 24000$, $\omega_{pFe}t = 74$

Ion Density $n_i(x)$

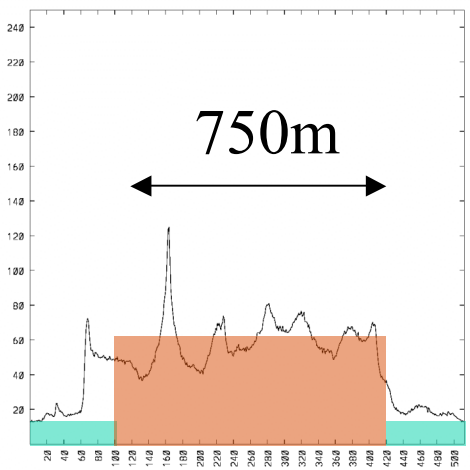

x / ρ_e

Electron Parallel Distribution $f_e(v_{\|})$

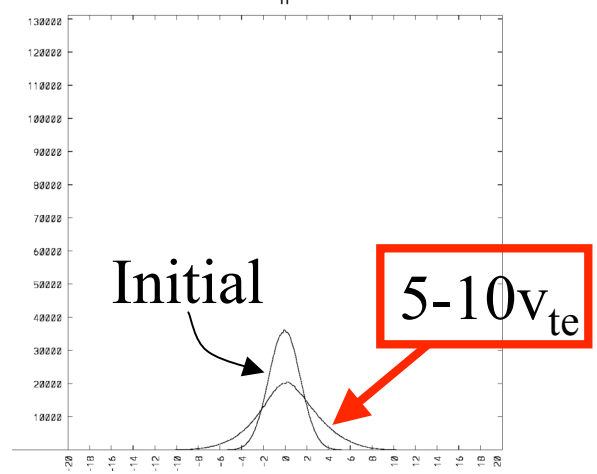

$v_{\|} / v_{te}$

Ion Perpendicular Distribution $f_i(v_{\perp})$

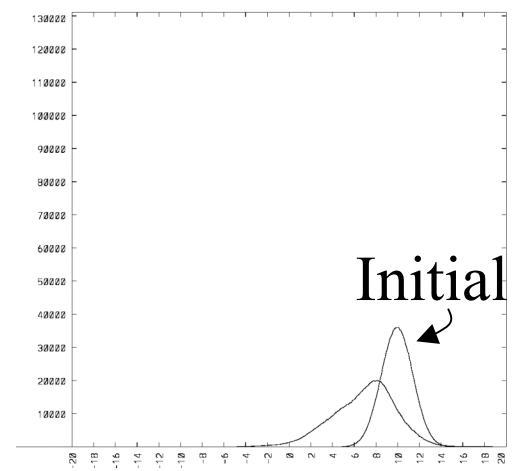

v_y / v_{ti}

$\rho_e = c/\omega_{pe}$; $\rho_i = 64\ \rho_e = 15$m

Electrostatic Particle Simulation

- Wave Field at $\omega_{pe}t = 24000$, $\omega_{pFe}t = 74$

Ion Density $n_i(x)$

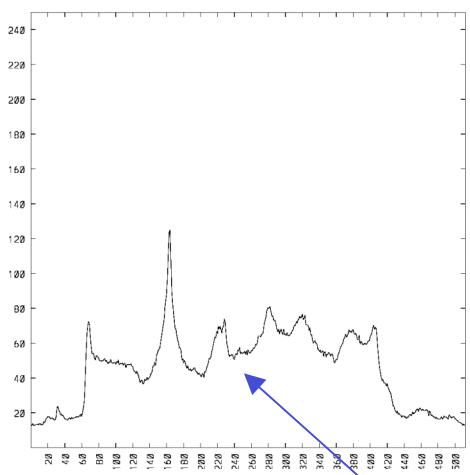

x / ρ_e

Electron Density $n_e(x)$

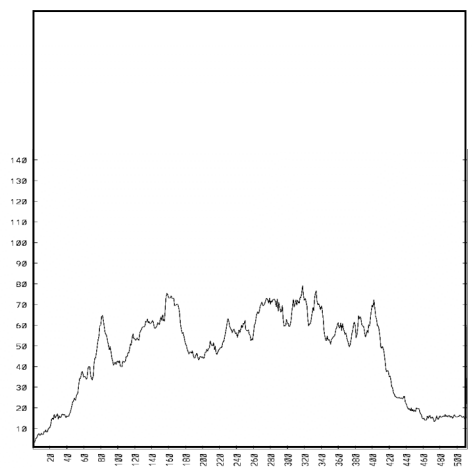

x / ρ_e

Electrostatic Potential f (x,y)

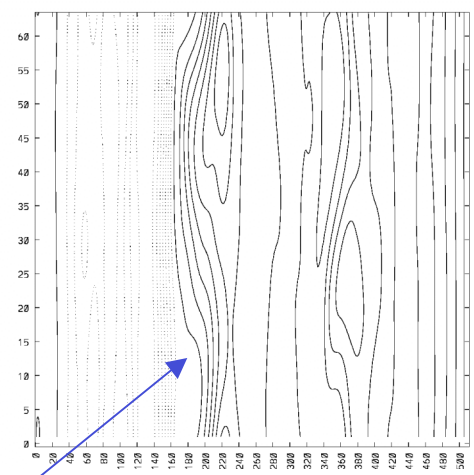

y / ρ_e

x / ρ_e

Mode localized in heavy ion layer

Consequences for Aurora

- Electrons are heated symmetrically
- High energy electron tail forms with thermal speed 5-10 times larger than the initial distribution

$$\boxed{1\ \text{eV} \Rightarrow 25\text{-}100\ \text{eV}}$$

- Result suggests that modified two-stream instability could energize electrons to energies required for enhanced auroral emissions

References

Incoherent Scatter Observations of Thin Ionization Layers at Sondrestrom, W. A. Bristow and B. J. Watkins, *J. Atmosph. Terr. Phys., 18,* 873-894, 1993

Enhanced Aurora, T. J. Hallinan, H. C. Stenbaek-Nielsen and C. S. Deehr, *J. Geophys. Res*., **90**, 8461-8475, 1985.

The Role of Electric Field and Neutral Wind Direction in the Formation of Sporadic E-Layers, T. Nygrén, L. Jalonen, and J. Oskman, T. Turunen, *J. Atmos. Terr. Phys*., **46**, 373-381, 1984.

Density Profiles of Sporadic E-Layers Containing Two Metal Ion Species, T. Nygrén, L. Jalonen, and A. Huuskonen*, J. Atmos. Terr. Phys*., **46**, 885-893, 1984.

Observations of Thin Auroral Ionization Layers by EISCAT in Connection with Pulsating Aurora, J.-E. Wahlund and H. J. Opgenoorth, and P. Rothwell, *J. Geophys. Res.,* **94**, 17,223-17,233, 1985.

Theory and Simulation of Turbulent Heating by the Modified Two-Stream Instability, J. B. McBride, E. Ott, J.P. Boris, and J.H. Orens, *Phys. Fluids*, **15**, 2367-2379, 1972.

Reprint Request

Name Address